Vol 10 Suppl., July 2001
1009-1963/2001/10(Suppl.)/0S70-06
Chinese Physics
© 2001 Chin. Phys. Soc.
and IOP Publishing Ltd

SELF-ASSEMBLY AND POLARIZABILITY OF CAPPED CdS NANOCRYSTALS ON SILICON SURFACES*

Ba Long(巴 龙)†, Zhang Yu(张 宇), and Lu Zu-hong(陆祖宏)
Laboratory of Molecular and Biomolecular Electronics, Southeast University, Nanjing 210096, *China*

(Received 20 April 2001)

The zinc-blende CdS nanocrystals with particle size less than 10nm were prepared in solution with a molecular surfactant. The particle surface was modified with capping molecules, bis(2-ethylhexyl) sulfosuccinate disodium salt (AOT) or hexametaphosphate (HMP). The colloid solution was deposited on silicon wafer and the assembly of these nanocrystals was studied by atomic force microscopy. It was found that the CdS/AOT formed a monolayer by simply dropping the colloid solution on silicon surface, while CdS/HMP exhibited 3D structure with prefered orientation in the similar deposition process. A dynamic electric force microscopy was performed and the polarizability was measured from the resonance of cantilever under applied alternating voltage between tip and substrate. The dielectric constant of CdS nanocrystal was estimated by comparing the different electric capacitance of Au and CdS nanocrystals.

Keywords: nanoparticle, self-assembly, scanning probe microscopy
PACC: 7320

I. INTRODUCTION

Synthesizing semiconductor nanocrystals and fabricating functional structures open up potential applications that bridge the gap between the quantum effect of single particles and the collective behavior of bulk material. Various microstructures of nanocrystals (0–3D superlattices, nanocrystal wires)[1−5] have been achieved through self-assembling process by carefully modifying the surface of particles and controlling the aggregation process. Fendler's group first assembled semiconductor nanoparticles to form self-organized structures by using Langmuir monolayer as template.[6] In order to assemble nanoparticles into ordered structures, various attempts such as modification of the particle surface, using a suitable solution environment, and controlling the deposition process have been employed to optimize interparticle and particle/substrate interaction. The electrostatic interaction between particles and nanoparticle/substrate has been studied for self-assembling nanoparticle structures and functional devices.[7−9] By bonding molecules onto the nanoparticle surface, these interactions can be tailored to construct large scale ordered structures.

Recent progresses in scanning probe microscopy provide opportunities to study the surface charge density and the local dipole moment. Various methods have been developed to show local electric charges or electric force gradients near the substrate surface within several nanometers.[10,11] With a similar method, the local charge and polarization of various materials have been studied and the lateral resolution can be refined to several tens of nanometers.[12,13] To reveal the charge and dielectric response of single semiconductor particles, we also use the electric force microscopy (EFM) to map the dielectric response of nanocrystal monolayer.

Various nanoparticle self-assembled ordered structures have been achieved by using the Langmuir monolayer, electropolymerized poly-N-vinylcarbazole template.[14,15] Here we present a study on the preparation of CdS nanocrystal surfaces modified by AOT and HMP, and the assembly of nanocrystals on silicon wafers. From the resonance of the cantilever under applied modulated voltage between tip and single particle, the dielectric constant of capped CdS nanocrystals was estimated from the capacitance of nanocrystals.

II. EXPERIMENTAL

AOT modified CdS nanocrystals were prepared using the similar method as reported.[16] AOT was dissolved in heptane, then add water to a ratio $[H_2O]$:[AOT]=8. By magnetical stirring a microemulsion was formed. The microemulsion kept its original optical homogeneity after dropping of Cd^{2+} so-

*Project supported by the "Nanoelectronics" Key Project (69890200) of National Natural Science Foundation of China.
†Corresponding author, E-mail:balong@seu.edu.cn

lution. The color thickened and reverse micelle solution formed after quickly adding microemulsion solution containing S^- with $[Cd^{2+}]$:$[S^-]$=1.44. The yellow floccule occurs at the interface between heptane and dimethyl formamide(DMF) after dropping a proper amount of DMF. These flocculated particles were cleaned by centrifugation and filtration, then the collected sufactant-stablized CdS nanocrystals was dissolved in chloroform with a concentration of 1.67×10^{-3}mol/L.

The CdS nanocrystals capped by HMP^- were prepared by simply blending the aqueous solutions of $Cd(NO_3)_2$ and HMP with Na_2S under stirring. The concentrations of $Cd(NO_3)_2$, Na_2S and HMP are 1:1:1. The concentration of the resulting CdS colloidal solution is 5×10^{-4}mol/L. The as-prepared colloidal solution were mounted on a copper mesh through dipping and observed by transmission electron microscopy (TEM) (JEOL-2000EX). The modified CdS colloids were deposited by a dipping and drying procedure on to n-type(100) silicon, which has been previously treated by HF solution. Solutions with various concentrations were selected for comparison. The as-prepared CdS/AOT was diluted 2, 5 and 10 times, and CdS/HMP was diluted 1,2 and 3 times for comparison. All samples have been deposited on silicon wafers and various evaporation rates (from 1min to 5min for CdS/AOT, 1h to 4h per 0.1mL for CdS/HMP) have been tried.

The Digital Instrument Nanoscope IIIa AFM was used to view the topography of the CdS particle aggregation on the silicon wafers. The TiN coated ultrasharp silicon cantilever (Silicon MDT) was used in EFM experiment. The dynamic electric response of the cantilever was measured as illustrated in Fig.1. By applying an alternating bias voltage between tip and sample, the resonance of cantilever can be detected by a lock-in amplifier.

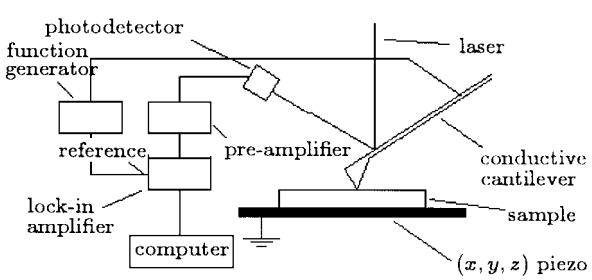


Fig.1. Configuration diagram of the dynamic electrostatic force microscopy.

Since surface water layer may screen the surface charge and deteriorate the cantilever resonance condition, it is important to dry the sample (baked at 70°C for 5h) after evaporation and the experiment shall be operated in a dry environment (relative humidity <10%). The lift mode was applied for all dynamic EFM imaging with 10nm lift height. The resonance frequency of cantilever is 59.32kHz.

In order to get a more reliable dielectric constant of CdS nanocrystals, we deposited Au and CdS nanocrystals on the same substrate (first deposition of diluted Au colloid aqueous solution, then deposition of CdS), as suggested by Krauss and Brus.[12] It is expected to determine the dielectric constant by comparing the contrast of two kinds of particles with large difference in dielectric constans.

III. RESULTS AND DISCUSSIONS

The CdS nanocrystals capped with AOT and HMP aggregation morphology is shown in Fig.2. Figure 2(a) is TEM image and electron diffraction pattern of CdS/AOT nanocrystals, Figure 2(b) is TEM image of CdS/HMP nanocrystals. The bright regions are CdS particles. It can be seen that the distribution

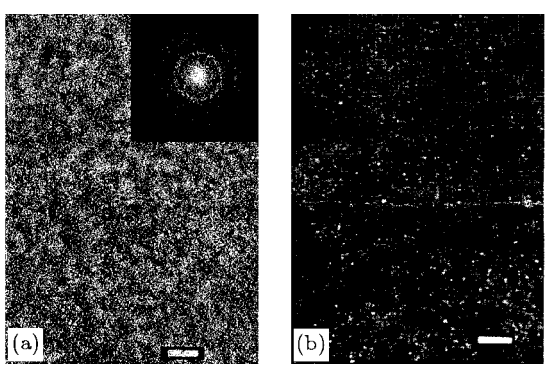


Fig.2. (a) TEM image and electron diffraction pattern of CdS nanocrystals capped by AOT, scale bar is 50nm. (b) TEM image of CdS nanocrystals capped by HMP, scale bar is 100nm, bright regions are CdS nanocrystals.

of CdS/ AOT particles is uniform, and the particle size is much larger than the CdS/HMP particles(around 10nm). The size of CdS/HMP particles is several nanometers and the particles are well separated by HMP. Sharp diffraction rings of CdS/AOT show that nanocrystals keep cubic zinc blende structure. Figure 3(a) and 3(b) are AFM images of the assembled CdS nanocrystals on the silicon wafer. From Fig.3(a), each particle can be identified and the particle size appears to be 20–30nm. This discrepancy is caused by tip-particle convolution and the influence of the molecule-capping layer on the particle surface. Tip curvature

radius of our cantilever is less than 35nm. Figure 3(b) is the larger scale image of CdS/HMP particles aggregated into 3D structures. The particle size appearing in AFM image is similar to that of CdS/AOT. The difference of particle size and aggregation feature in TEM image could not be seen in AFM images.

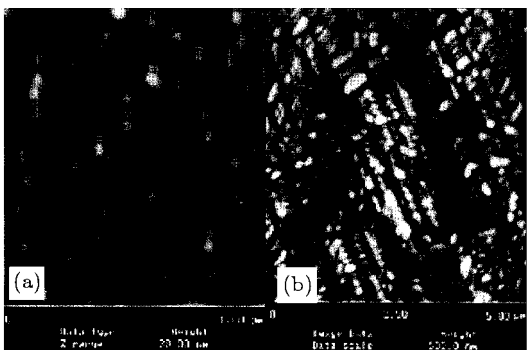


Fig.3. AFM image of CdS/AOT and CdS/HMP nanocrystals assembled on silicon wafer. (a) Image area $\sim (1\mu m)^2$ (b) image area $\sim (5\mu m)^2$

The molecular structure of AOT and HMP are shown in Fig.4. In aqueous solution, the sodium ion dissolves and AOT is negatively charged. The CdS nanocrystal surface is rich in Cd^{2+} ions. The AOT^- or HMP^- molecules are attracted to the nanocrystal surface by Coulombic interaction. During the reaction between Cd^{2+} and S^{2-}, the nucleation site and the growth rate of CdS nanocrystals are balanced by molecules bonded to CdS atomic clusters and its growth is finally screened. It are the surface stabilizing molecules and their concentration in solution that dominate the size and the surface state of particles. The size and the surface charge of each colloidal particle decide the inter-particle potential, which plays the main role in the self-assembling process.

We also exammed the particles on silicon surfaces from diluted solutions of different concentration. We found that the CdS/AOT nanocrystals can form a monolayer at 1.67×10^{-4}mol/L and an evaporation rate of 5min/0.1mL, while CdS/HMP nanocrystals can not form monolayers at any concentrations and evaporation rates. From Fig.3, it can be seen that the CdS/AOT sample shows an assembled monolayer on silicon surfaces with flat regions not less than 1μm in size (Fig.3(a)), the CdS/HMP sample shows 3D humps at the concentration of 5×10^{-4}mol/L and evaporation rate of 1h/0.1mL. At more diluted concentration, these nanocrystals tend to form dispersive clusters rather than a monolayer. Figure 3(b) shows that the particles aggregated in a preferential orientation, with inter-stripe period of about 100nm, larger than the size of a single particle as observed in diluted samples. The above observation shows that CdS nanocrystals capped by AOT are homogeneously separated, while that capped by HMP tend to form clusters. TEM shows CdS/HMP are well dispersed with larger interparticle distance, while image of CdS/AOT shows that the particles are closely combined and somewhat larger in particle size.

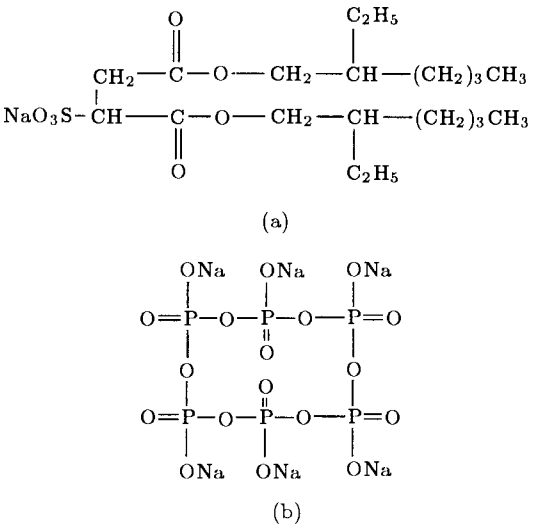


Fig.4. Molecular structure of AOT(a) and HMP(b).

To measure the polarization of a single particle, a bias was applied between tip and substrate. In this study, the contribution of electric carrier within n-type Si is simplified to effective charge in the substrate. The force induced by electric charge between tip and sample is the sum of capacitive force and Coulombic force. A simplified model takes a point charge q on sample surface to interact with AFM tip. If there is an insulator layer on substrate, the image charge within this layer may also be considered. These charges and the induced charge in tip contribute to the force between tip and sample. The electric force under applied alternate voltage can be expressed as:

$$F_e = \frac{1}{2}\frac{\partial C}{\partial z}\left(V_{dc} + \frac{q_2}{C} + V_{ac}\sin(\omega t)\right)^2 + \frac{qC\left(V_{dc} + \frac{q_2}{C} + V_{ac}\sin(\omega t)\right)}{4\pi\varepsilon_0 z^2} + \frac{q_1 C\left(V_{dc} + \frac{q_2}{C} + V_{ac}\sin(\omega t)\right)}{4\pi\varepsilon_0\left(z + \frac{2h}{\varepsilon_1}\right)^2}$$

$$
\begin{aligned}
=&\frac{1}{2}\frac{\partial C}{\partial z}\left(V_{\mathrm{dc}}+\frac{q_2}{C}\right)^2\\
&+\frac{\partial C}{\partial z}\left(V_{\mathrm{dc}}+\frac{q_2}{C}\right)V_{\mathrm{dc}}\sin(\omega t)\\
&+\frac{1}{2}\frac{\partial C}{\partial z}V_{\mathrm{ac}}^2\sin^2(\omega t)+\frac{qC\left(V_{\mathrm{dc}}+\frac{q_2}{C}\right)}{4\pi\varepsilon_0 z^2}\\
&+\frac{q_1 C\left(V_{\mathrm{dc}}+\frac{q_2}{C}\right)}{4\pi\varepsilon_0\left(z+\frac{2h}{\varepsilon_1}\right)^2}\\
&+\left(\frac{qC}{4\pi\varepsilon_0 z^2}+\frac{q_1 C}{4\pi\varepsilon_0\left(z+\frac{2h}{\varepsilon_1}\right)^2}\right)\sin(\omega t), \quad (1)
\end{aligned}
$$

where V_{dc} is the direct bias voltage applied to cantilever, z is the distance from tip to the sample surface, V_{ac} and ω is the amplitude and frequency of the applied alternating bias voltage. C is the capacitance between tip and sample. q, q_1 and q_2 are local surface charges and the induced charge in the substrate and tip, respectively. h and ε_1 are the thickness and the dielectric constant of the insulator layer on the substrate surface. From the above equation, the force fluctuating at ω and 2ω can be expressed as:

$$
\begin{aligned}
F_{\mathrm{e}}(\omega)=&\left(\frac{\partial C}{\partial z}\left(V_{\mathrm{dc}}+\frac{q_2}{C}\right)+\frac{qC}{4\pi\varepsilon_0 z^2}\right.\\
&\left.+\frac{q_1 C}{4\pi\varepsilon_0\left(z+\frac{2h}{\varepsilon_1}\right)^2}\right)\sin(\omega t), \quad (2)
\end{aligned}
$$

$$
F_{\mathrm{e}}(2\omega)=\frac{1}{2}\frac{\partial C}{\partial z}V_{\mathrm{ac}}^2\cos(2\omega t). \quad (3)
$$

Considering the contact potential φ between tip and sample, the V_{dc} shall be $V_{\mathrm{dc}}+\varphi$. From the force at ω, the surface charge can be detected, while the capacitance gradient is reflected in the force at 2ω. In our experiment, the SiO_2 layer on silicon substrate is dissolved for simplicity and q_1 will not be considered in the following discussion.

The capacitance between tip and substrate depends on the shape of the tip, the dielectric constant, the size and the shape of the particle located between tip and substrate. The shift of the resonance frequency to the drive frequency(ω) is proportional to the negative force gradient. The signal we used to map the surface charge and dielectric resonance is the out-put amplitude from the lock-in amplifier. It is known that the vibration amplitude change ΔA is proportional to the force gradient. From Equation 3, the resonance force at 2ω is only proportional to the differential capacitance. The capacitance between tip and substrate is sensitive to surface absorption layer, particle size and particle/substrate contact. The capacitance between tip and metallic substrate with air and particle in the gap can be expressed as serial capacitance of air gap and particle. In the case of semiconductor substrate, this capacitance shall include a part induced by space carrier near substrate surface. In the above experiment, we have used heavily doped n-type silicon wafer as the substrate, thus ignored the difference of capacitance induced from carrier moving near the surface. So in the case of constant tip/substrate or tip/particle separation, the amplitude change only reflected the local change of dielectric constant. By comparing the amplitude change between Au and Si or CdS and Si, the dielectric constant of CdS can be measured, since the large dielectric constant difference between Au and CdS causes large amplitude contrast in the $F(2\omega)$ image. For a metal particle, the potential on it is close to that on silicon the surface where the particle contacts. If we simplify the capacitance between tip and substrate to that of a parallel capacitor, the differential capacitance can be expressed as $\mathrm{d}C/\mathrm{d}z = A/\varepsilon_1 \cdot 1/(z/\varepsilon_1 + d/\varepsilon_2)^2$, A, z, d, ε_1 and ε_2 being the equivalent area, tip/substrate (particle) separation, particle size, dielectric constant of air and particle, respectively. When the dynamic EFM was operated under the tapping mode, the lift mode maintained the tip at a constant fluctuation starting height over scanned area. Though the actual shape of tip and nanocrystal will modify the capacitance-separation relation($C - z^{1.2}$),[13] if two particles have similar size, its difference on $F(2\omega)$ is only affected by the dielectric constant ε_2. So the fluctuation amplitude driven by the applied ac bias voltage shall be smaller for lower dielectric constant.

To acquire EFM image, topography and electric resonance signals were imaged by alternately scanning the cantilever over the sample surface in height and lift mode, there and topography and electric force images can be collected simultaneously. Figure 5 is the topography, charge and dielectric image taken from nanocrystal CdS and Au assembled on Si wafer. Different dc bias voltages were applied to the sample. When the applied bias is set to zero or $V_{\mathrm{dc}}+\varphi$ is kept to zero, the $F(\omega)$ only reflect surface charge. The $F(2\omega)$ image(Figure 5(c)) was otained at the same place.

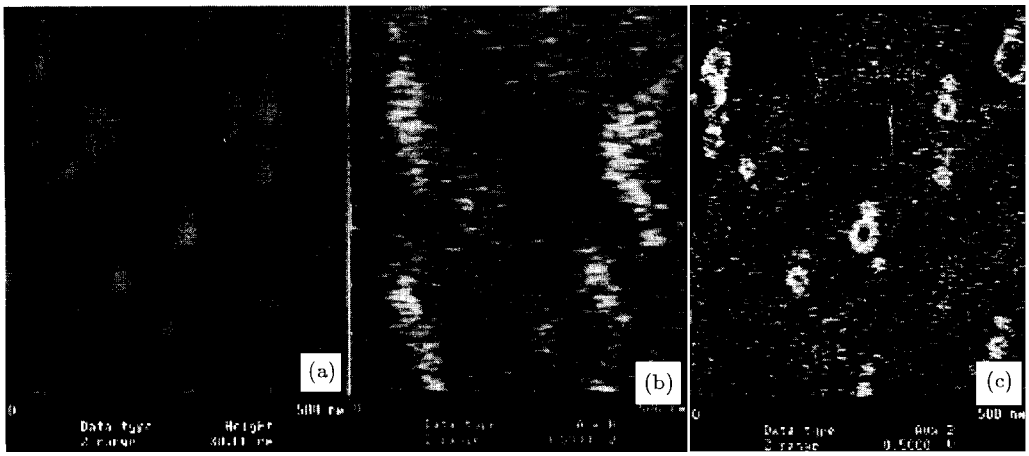


Fig.5. (a) Topographic image of AOT capped CdS nanoparticle monolayer on silicon surface, (b) charge image from cantilever resonance at ω with bias voltage 2V to the sample, (c) dielectric image from cantilever resonance at 2ω with no bias voltage to sample; ac signal to tip is 2V 4KHz, lift mode, lift height is 10nm.

It is noticed that after a positive bias was applied, the bright contrast in $F(\omega)$ image corresponding to position of both Au and CdS nanocrystals is caused either by polarized dipoles or charge transfer from substrate, which depends on whether there exists electric contact or effective charge transfer between particle and conductive substrate. By varying the applied bias, it was noticed that the contrast of $F(\omega)$ image decreased as bias was reduced and no contrast was seen at 0V bias for CdS/AOT, which means that no residual charge exists on the particles. It could be understood that the charge on CdS nanoparticles should be polarized dipole, since the relaxation of electric charge on a nanocrystal will take several seconds to several minutes. In the case of CdS/HMP, we have observed that $F(\omega)$ image does not totally fade out at the 0V bias, it appears that there is a 0.3V charge transfer between substrate and CdS, and no delay effect was observed. For simplicity, in the following we discuss only the results for CdS/AOT.

Figure 5 is the images of the topography (Figure 5(a)), $F(\omega)$ (Figure 5(b)) and $F(2\omega)$ (Figure 5(c)). From $F(\omega)$ and $F(2\omega)$ images, it can be identified that all bright particles in $F(\omega)$ do not coincide with that shown in the $F(2\omega)$ image, as indicated by arrows. This difference tells that it shall not be enough to identify Au and CdS nanoparticles from surface charge images, since surface charges on different particles could be at a similar level. The dielectric images (Figure 5(c)) of Au and CdS nanocrystal shows that there are different types of contrast. Most particles exhibit slightly higher contrast comparing to the area of substrate, while some particles (their sizes are a little bit larger) exhibit very high contrast at their fringes and much lower contrast in their center(indicated by arrow in Figure 5(c)). The very high fluctuation amplitude at the fringe of nanocrystal can be attributed to the large change of capacitance gradient when tip jumping from substrate to particle.

It is difficult to estimate the capacitance gradient from the amplitude change with convincible accuracy, since it is not easy to achieve accurate measurements of the Young's modulus and the quality factor. But we can get an estimation of the dielectric constant of CdS nanocrystal if the first order approximation of force gradient on the change of fluctuation amplitude is acceptable. By comparing the lower amplitude in the center of several particles(CdS) to the slightly higher amplitude of the other particles(Au), and using a relation of $C - z^{1.2}$, we get the rough value of the dielectric constant of CdS nanocrystal.

The CdS nanocrystal exhibits lower dielectric constant compared that of bulk material as shown in the previous study.[17] The molecular capping layer might also affect the effective dielectric constant of CdS nanocrystals. By assuming a much larger dielectric constant of Au, and set z and d to 10nm and 20nm, respectively, the dielectric constant of dark region was calculated to be 4 ± 2. The ε of bulk CdS is 5.6. In spite of the deviations caused by either the noise in the amplitude signal or the ambient environment, the results can tell the tendency of size effect. Using a carefully calibrated cantilever can help to know the dependence of capacitance on tip/substrate separation; controlling the experiment atmosphere will retard the noisy fluctuation of the cantilever. Such efforts could

make more accurate measurements possible.

IV. CONCLUSION

The CdS nanocrystals were prepared from reaction between Cd^{2+}, S^{2-} with AOT, HMP as surface stabilizing molecules. By control of particle concentration and evaporation speed, CdS/AOT nanocrystals can form a monolayer, while 3D aggregation with prefered orientation was found for CdS/HMP samples. Both static and dynamic polarization of nanocrystals were studied by using a dynamic-EFM. The surface charge image acquired over assembled nanocrystals on a silicon wafer shows that the capping layer of AOT molecules could effectively insulate the charge transfer from substrate to particles. The dielectric resonance measurement shows that the dielectric constants of CdS nanocrystals capped by AOT or HMP have not been dramatically modified within our experiment accuracy. Dielectric resonance measurements enable promising studies of the dynamic polarization behavior of nanocrystals at low frequency with different surface modifications, and to study the effect of inter-particle dipoles on the self-assembling process.

References

[1] Colvin V L, Goldenstein A N and Alivisatos A P 1992 *J. Am. Chem. Soc.* **114** 5221

[2] Heath J R 1995 *Science* **270** 1315
Murray C B, Kagan C R and Bawendi M G 1995 *Science* **270** 1335

[3] Fendler J H *Membrane-Mimetic Approach to Advanced Materials* 1994 (Berlin: Springer-Verlag)

[4] Martin C R 1994 *Science* **266** 1961

[5] Mann S 1993 *Nature* **365** 499

[6] Zhao X K, Yang J, McCormick L D and Fendler J H 1992 *J. Phys. Chem.* **96** 9933

[7] Salata O V, Dobson P J, Hull P J and Hutchison J L 1994 *Adv. Mater.* **6** 772

[8] Bezryadin A, Dekker C and Schmid G 1997 *Appl. Phys. Lett.* **71** 1273

[9] Torimoto T, Yamashita M, Kuwabata S, Sakata T, Mori H and Yoneyama H 1999 *J. Phys. Chem.* B **103** 8799

[10] Yokoyama H, Inoue T and Itoh J 1994 *Appl. Phys. Lett.* **65** 3143

[11] Hidaka T, Maruyama T, Saitoh M, Shimizu M, Shiosaki T, Wills L A, Hiskes R, Dicarolis S and Amano J 1996 *Appl. Phys. Lett.* **68** 2358

[12] Krauss T D and Brus L E 2000 *Phys. Rev. Lett.* **83** 4840

[13] Krauss T D and Brus L E 2000 *Mater. Sci. Eng.* **69-70** 289

[14] Liu J F, Yang K Z and Lu Z H 1997 *J. Am. Chem. Soc.* **119** 11061

[15] Pan Z Y, Shen G J, Zhang L G, Lu Z H and Liu J Z 1997 *J. Mater. Chem.* **7** 531

[16] Steigerwald M L, Alivisatos A P, Gibson J M, Harris T D, Kortan R, Muller A J, Thayer A M, Duncan T M, Douglass D C and Brus L E 1988 *J. Am. Chem. Soc.* **110** 3046

[17] Abdulkhaadar M and Thomas B 1995 *Physica Status Solidi* A **150** 755